

Chiral nonperturbative approach to the isoscalar s-wave $\pi\pi$ interaction in a nuclear medium

H.C. Chiang ¹, E. Oset and M.J. Vicente-Vacas

*Departamento de Física Teórica and IFIC
Centro Mixto Universidad de Valencia-CSIC
46100 Burjassot (Valencia), Spain*

Abstract

The s-wave isoscalar amplitude for $\pi\pi$ scattering in a nuclear medium is evaluated using a nonperturbative unitary coupled channels method and the standard chiral Lagrangians. The method has proved successful to describe the $\pi\pi$ properties in the scalar isoscalar channel up to 1.2 GeV giving rise to poles in the t matrix for the $f_0(980)$ and the σ . The extension of the method to the nuclear medium implies not only the renormalization of the pions in the medium, but also the introduction of interaction terms related to contact terms in the $\pi N \rightarrow \pi\pi N$ interaction. Off shell effects are also shown to be important leading to cancellations which reduce the coupled channel integral equations to a set of algebraic equations. As the density increases we find a reduction of strength below the σ region and a certain accumulation of strength at energies around pion threshold. Our results, based on chiral Lagrangians, provide similar results to those obtained with phenomenological models which impose minimal chiral constraints.

¹Permanent address: Institute of High Energy Physics. Chinese Academy of Sciences, Beijing, 100039, China

1 Introduction.

The $\pi\pi$ interaction in a nuclear medium in the $J = T = 0$ channel (σ channel) has stimulated much theoretical work lately. It was realized that the attractive p-wave interaction of the pions with the nucleus led to a shift of strength of the $\pi\pi$ system to low energies and eventually produced a bound state of the two pions around $2m_\pi - 10 \text{ MeV}$ [1]. This state would behave like a $\pi\pi$ Cooper pair in the medium, with repercussions in several observable magnitudes in nuclear reactions [1]. The possibility that such effects could have already been observed in some unexpected enhancement in the $(\pi, 2\pi)$ reaction in nuclei [2] was also noticed there. More recent experiments where the enhancement is seen in the $\pi^+\pi^-$ channel but not in the $\pi^+\pi^+$ channel [3] have added more attraction to that conjecture.

Yet, it was early realized that constraints of chiral symmetry might affect those conclusions [1]. In order to investigate the influence of chiral constraints in $\pi\pi$ scattering in the nuclear medium two different models for the $\pi\pi$ interaction were used in [4]. One of them from [5] did not satisfy the chiral constraints, while another one from [6] produced an amplitude behaving like m_π in the limit of small pion masses. The conclusion of [4] was that, although in the chirally constrained model the building up of $\pi\pi$ strength at low energies was attenuated, it was still important within the approximations done in their calculations. The latter ones used some approximations, amongst others, the use of only Δh excitation with zero Δ width to build up the π nuclear interaction. Warnings were also given that results might depend on the off shell extrapolation of the $\pi\pi$ scattering matrix.

Further refinements were done in [7], where the width of the Δ and coupling to $1p1h$ and $2p2h$ components were considered. The coupling of pions to the ph continuum led to a dramatic re-shaping of the $\pi\pi$ strength distribution, but the qualitative conclusions about the accumulated strength at low energies remained.

In ref. [8] the importance of the coupling to the ph components was re-confirmed and the use of more accurate models for the $\pi\pi$ interaction, as the Jülich model based on meson exchange [9], did not change the conclusions on the enhanced $\pi\pi$ strength at low energies. However, the use of a linear and nonlinear models for the $\pi\pi$ interaction, satisfying the chiral constraints at small energies, led to quite different conclusions and showed practically no enhancement of the $\pi\pi$ strength at low energies. The same conclusions were reached using the Jülich model with a subtracted dispersion relation so as to satisfy the chiral constraints. The latter model employed the Blakenbecler-Sugar equation in which the 2π intermediate states were placed on-shell. The conclusion of this paper was that the imposition of chiral constraints in the $\pi\pi$ amplitude prevented the pairing instabilities shown by the other models not satisfying those constraints.

In a further paper [10] the authors showed, however, that the imposition of the chiral constraints by themselves did not prevent the pairing instabilities

and uncertainties remained related to the off-shell extrapolation of the $\pi\pi$ amplitude and the possible ways to implement the minimal chiral constraints. The situation, as noted in [10] is rather ambiguous, but the studies done have certainly put the finger in the questions that should be properly addressed: chiral symmetry, off-shell extrapolations, unitarity, etc.

After the above discussions it looks quite intuitive to think that the use of chiral Lagrangians, and chiral perturbation theory, where the $\pi\pi$ interaction at low energies has been thoroughly studied [11], should be the appropriate framework to look at this problem. However, the scalar sector shows additional problems. The $J = T = 0$ $f_0(980)$ resonance does not show up in chiral perturbation theory, and even the σ pole does not show up in this perturbative approach. Since one is dealing here with the shift of the " σ strength" to lower energies it looks most advisable to start with a theory where the σ shows up neatly in the $\pi\pi$ interaction. Fortunately, two recent independent approaches using the Gasser and Leutwyler chiral Lagrangians, which implement unitarity in an exact way, have succeeded in reproducing the low energy $\pi\pi$ phase shifts while at the same time generating a " σ " pole in the $\pi\pi$ T matrix in the II sheet of the complex plane [12, 13].

In ref. [12] the method of the inverse amplitude of [14] was used where elastic unitarity in the $\pi\pi$ channel is imposed. The method obtains good results for the low energy $\pi\pi$ interaction in all channels. It, however, fails to obtain the $f_0(980)$ and $a_0(980)$ resonances in the scalar $T = 0$ and $T = 1$ channels respectively, but the σ pole in $J = T = 0$ is obtained.

In ref. [13] unitarity in coupled channels is built from the beginning with $\pi\pi$ and $K\bar{K}$ in the scalar, isoscalar sector and $\pi\eta, K\bar{K}$ for $J = 0, T = 1$. The phase shifts and inelasticities are well reproduced up to about 1.2 GeV. The σ and $f_0(980)$ resonances appear as poles in the $J = T = 0$ channel and the $a_0(980)$ appears as a pole in $J = 0, T = 1$. The coupling of channels was found essential to produce the $f_0(980)$ and $a_0(980)$ resonances, while the σ pole was not much affected by the coupling of the pions to $K\bar{K}$. This would make the approaches of [12] and [13] similar at energies around the σ pole and, indeed, the results in that region are practically equal. This has been made more explicit in a recent paper where the two methods discussed above are unified into a more general scheme [15]. A different perspective of this method is also given in [16].

The existence of these chiral nonperturbative methods offers unique opportunities to tackle the problem of the scalar isoscalar $\pi\pi$ interaction in the nuclear medium and this is the purpose of the present work. We follow here the approach of ref. [13], where one of the problems pointed above, the off shell extrapolation, was worked out with detail. This, together with the automatic implementation of chiral symmetry and its breaking, given by the Gasser and Leutwyler chiral Lagrangians, allows us to face the problems mentioned above from a different perspective, where chiral symmetry, off shell extrapolation, etc., are directly associated to the structure of the chiral Lagrangians.

In constructing the $\pi\pi$ amplitude in the medium we will show that chiral

symmetry introduces new terms which do not appear in the approaches discussed above and which lead to cancellations of other terms coming from the off shell extrapolation of the $\pi\pi$ amplitude.

The results show some enhancement of the $\pi\pi$ strength at low energies, similar to what is found in different approaches, particularly those imposing the minimal chiral constraints. The work serves to establish closer links with chiral dynamics and justify certain prescriptions proposed in the past.

2 Non perturbative chiral approach to $\pi\pi$ scattering in the isoscalar isovector channel.

We briefly summarize here the ingredients of ref. [13] which will be used here. The approach uses the coupled channels Lippmann Schwinger (LS) equation, although with relativistic meson propagators (equivalent to Bethe Salpeter equations). We take the states $|1\rangle = (K\bar{K}, T=0)$, $|2\rangle = |\pi\pi, T=0\rangle$ and the LS equations read as

$$T_{ij} = V_{ij} + \overline{V_{il}G_{lu}T_{lj}} \quad (1)$$

where V_{ij} , the potential or Kernel of the LS equations, is obtained from the lowest order chiral Lagrangians [11].

$$L_2 = \frac{1}{12f^2} \langle (\partial_\mu\Phi\Phi - \Phi\partial_\mu\Phi)^2 + M\Phi^4 \rangle \quad (2)$$

where the symbol $\langle \rangle$ indicates the trace in flavour space of the $SU(3)$ matrices, f is the pion decay constant and Φ , M are $SU(3)$ matrices given by

$$\Phi \equiv \frac{\vec{\lambda}}{\sqrt{2}}\vec{\phi} = \begin{pmatrix} \frac{1}{\sqrt{2}}\pi^0 + \frac{1}{\sqrt{6}}\eta_8 & \pi^+ & K^+ \\ \pi^- & -\frac{1}{\sqrt{2}}\pi^0 + \frac{1}{\sqrt{6}}\eta_8 & K^0 \\ K^- & \bar{K}^0 & -\frac{2}{\sqrt{6}}\eta_8 \end{pmatrix}, \quad (3)$$

$$M = \begin{pmatrix} m_\pi^2 & 0 & 0 \\ 0 & m_\pi^2 & 0 \\ 0 & 0 & 2m_K^2 - m_\pi^2 \end{pmatrix}.$$

In the mass matrix, M , we have taken the isospin limit ($m_u = m_d$).

The elements of V_{ij} in the s-wave and $T=0$ needed here are given in [13] by

$$\begin{aligned}
T &= 0 \\
V_{11} &= - \langle K\bar{K} | \mathcal{L}_2 | K\bar{K} \rangle = -\frac{1}{4f^2}(3s + 4m_K^2 - \sum_i p_i^2) \\
V_{21} &= - \langle \pi\pi | \mathcal{L}_2 | K\bar{K} \rangle = -\frac{1}{3\sqrt{12}f^2}(\frac{9}{2}s + 3m_K^2 + 3m_\pi^2 - \frac{3}{2}\sum_i p_i^2) \\
V_{22} &= - \langle \pi\pi | \mathcal{L}_2 | \pi\pi \rangle = -\frac{1}{9f^2}(9s + \frac{15m_\pi^2}{2} - 3\sum_i p_i^2)
\end{aligned} \tag{4}$$

In eq. (1) the term \overline{VGT} stands for the integral

$$\overline{VGT} = \int \frac{d^4q}{(2\pi)^4} V(k_1, k_2, q) G(P, q) T(q; k'_1, k'_2) \tag{5}$$

where $k_1, k_2(k'_1, k'_2)$ are the initial (final) momenta of the mesons, $P = k_1 + k_2 = k'_1 + k'_2$ is the total momentum of the meson-meson system and q is the loop variable in the diagrams implicit in eq. (1) which are depicted in fig. 1.

$G(P, q)$ is now the product of the two meson propagators

$$G_{ii} = i \frac{1}{q^2 - m_{1i}^2 + i\epsilon} \frac{1}{(P - q)^2 - m_{2i}^2 + i\epsilon} \tag{6}$$

The on shell values of V_{ij} from eq. (4) are obtained substituting $p_i^2 = m_i^2$. The off shell extrapolation is then given by

$$V_{off} = V_{on} + \beta \sum_i (p_i^2 - m_i^2) \tag{7}$$

This peculiar off shell dependence has a practical consequence which converts the integral LS equations into ordinary algebraic equations. This is discussed in detail in ref. [13] but can be envisaged here quickly in the following way. Take a one loop diagram in the series of fig. 1 which will involve V_{off}^2 . This latter quantity can be written as

$$V^2 = V_{on}^2 + 2\beta V_{on} \sum_i (p_i^2 - m_i^2) + \beta^2 \sum_{ij} (p_i^2 - m_i^2)(p_j^2 - m_j^2). \tag{8}$$

Take the second term of the right hand side of eq. (8). The term $p^2 - m^2$ just kills one of the propagators in G of eq. (6). The remaining quantity can be easily integrated and gives a term of the type $V_{on} q_{max}^2$, where q_{max} is the cut off in the three momentum. The interesting thing to observe is that this term has the structure of the tree level term in the series, V_{on} , and hence is incorporated in the potential by means of a renormalization of the coupling f .

The use of the physical value of f incorporates effectively that term which, hence, must not be included in the calculation. Similarly the third term in eq. (8) can be reabsorbed in the coupling and the masses of the particles [13]. The practical consequence of this is that only the on-shell part of V_{ij} must be kept in the loop integral and, since they do not depend on q , they factorize outside the integral. The procedure can be repeated to higher order loops and thus the coupled LS equations become ordinary algebraic equations given by

$$T_{ik} = V_{ik} + V_{ij}G_{jj}T_{jk} \quad (9)$$

where

$$G_{jj} = i \int \frac{d^4q}{(2\pi)^4} \frac{1}{q^2 - m_{1j}^2 + i\epsilon} \frac{1}{(P - q)^2 - m_{2j}^2 + iG}$$

and hence, in matrix form

$$T = [1 - VG]^{-1}V \quad (10)$$

3 $\pi\pi$ scattering in the nuclear medium.

We will follow the previous approaches and will renormalize the pion propagators in G . In our coupled channel approach we should also renormalize the kaons, but given the fact found in [13] that the $K\bar{K}$ system does not affect much the low energy $\pi\pi$ regime, we shall keep the $K\bar{K}$ state in our coupled channel approach but without renormalization.

The pions are renormalized by allowing them to excite ph and Δh (the Δ with a finite width). At the level of one loop our renormalized amplitude would now contain the diagrams of fig. 2. Now let us take for instance the diagram of fig. 2b, cut it by a vertical line that cuts simultaneously the ph and the lower pion line, and keep the part of the diagram to the left of this vertical line. We obtain the diagram of fig. 3a. This diagram can be interpreted as one term contributing to the $\pi N \rightarrow \pi\pi N$ amplitude. However, even before chiral perturbation theory established an elegant and practical way to implement chiral symmetry and its breaking, it was already known that chiral symmetry required an extra term, shown in fig. 3b, which was readily obtained from a set of chiral Lagrangians [17]. Actually, one of the powerful consequences of chiral symmetry is that it establishes a relationship between amplitudes with different number of meson as external particles.

The set of the chiral Lagrangians is not unique and unitary transformations or redefinition of fields are possible [18]. The interesting thing is that, while each one of the terms in fig. 3 depends on the choice of Lagrangians, the sum of the two is independent of it. This is the case of the $\pi N \rightarrow \pi\pi N$ amplitude as well as any related observable magnitude. An example of it is found in the evaluation of the contribution of the nuclear virtual pion cloud to the pion selfenergy in the nuclear medium [19].

Chiral perturbation theory has allowed us to obtain the pion pole term of fig. 3a and the contact term of fig. 3b in an easier way than done in the past and also has allowed the possibility to extend these ideas to the octet of pseudoscalar mesons. As an example, the pion pole term and contact term for the $K\bar{K}\pi NN$ vertex were evaluated in [20], where the contribution of the virtual pion cloud to K^+ nucleus scattering was investigated.

The contribution of the diagrams of fig. 3a, 3b is the starting point of all models for the $\pi N \rightarrow \pi\pi N$ reaction [18, 21, 22, 23, 24] as well as in the $KN \rightarrow K\pi N$ reaction [25].

The requirements of chiral symmetry force us to include the contact term together with the pion pole term, and some cancellations appear that make the physical amplitudes respect the chiral limits, even in the presence of the nuclear medium. Indeed, in ref. [20] an exact cancellation was found between the contributions related to the pion pole and contact terms, while in ref. [19] the contribution was finite but vanished in the limit of $m_\pi \rightarrow 0$.

The former discussion has shown us that in addition to the terms depicted in fig. 2 we must add the terms depicted in fig. 4.

The Lagrangians involving the contact terms are obtained from the general chiral Lagrangians involving the pseudoscalar meson and baryon octets [11, 26, 27, 28]

$$\begin{aligned} \mathcal{L}_1^{(B)} &= \langle \bar{B} i \gamma^\mu \nabla_\mu B \rangle - M_B \langle \bar{B} B \rangle \\ &+ \frac{D+F}{2} \langle \bar{B} \gamma^\mu \gamma_5 u_\mu B \rangle + \frac{D-F}{2} \langle \bar{B} \gamma^\mu \gamma_5 B u_\mu \rangle, \end{aligned} \quad (11)$$

where B is a 3×3 matrix, which in our case, where only protons and neutrons are involved, reads as

$$B = \begin{pmatrix} 0 & 0 & p \\ 0 & 0 & n \\ 0 & 0 & 0 \end{pmatrix} \quad (12)$$

The three pion and a nucleon vertices, fig. 3b, are derived in [20] with the result

$$\begin{aligned} \mathcal{L}_1^{(B)} &= \frac{D+F}{2} (\bar{p} \gamma^\mu \gamma_5 u_\mu^{11} p + \bar{n} \gamma^\mu \gamma_5 u_\mu^{22} n \\ &+ \bar{n} \gamma^\mu \gamma_5 u_\mu^{21} p + \bar{p} \gamma^\mu \gamma_5 u_\mu^{12} n) \\ &+ \frac{D-F}{2} (\bar{p} \gamma^\mu \gamma_5 u_\mu^{33} + \bar{n} \gamma^\mu \gamma_5 u_\mu^{33} n), \end{aligned} \quad (13)$$

where u_μ^{ij} denotes the (i, j) matrix element of the u_μ matrix defined as

$$\begin{aligned} u_\mu &= -\frac{\sqrt{2}}{f} \partial_\mu \Phi \\ &+ \frac{\sqrt{2}}{12f^3} (\partial_\mu \Phi \Phi^2 - 2\Phi \partial_\mu \Phi \Phi + \Phi^2 \partial_\mu \Phi) \\ &+ O(\Phi^5). \end{aligned} \quad (14)$$

The $(D - F)$ term in eq. (13) does not contribute in our case since u_μ^{33} contains kaon fields.

By using the nonrelativistic reduction $\gamma^\mu \gamma_5 p_\mu \rightarrow -\vec{\sigma} \vec{p}$, the relevant terms which are needed in our approach are evaluated and they are shown in the Appendix.

We can also generalize these vertices to the case of $N\Delta$ transition by substituting [20]

$$\sigma_i \tau_j (\text{for nucleons}) \rightarrow \frac{f_{\pi N\Delta}^*}{f_{\pi NN}} S_i^\dagger T_j^\dagger \quad (15)$$

where S^\dagger, T^\dagger are the spin, isospin transition operators from 1/2 to 3/2.

As an example let us write the contribution of the left hand side vertex of the diagram of fig. 4a, which we depict in fig. 5a with labels for the momenta and a particular choice of pion charges. In the $\pi^+\pi^-$ CM frame ($\vec{k}_1 + \vec{k}_2 = 0$), and projecting over s-wave, we obtain the contribution of this vertex

$$-i\tilde{t}_{ph} = i\frac{1}{6f^4} \left(\frac{D+F}{2}\right)^2 \vec{q}_2^2 U_N(q_2) \quad (16)$$

where U_N is the Lindhard function for ph excitation [29]. The use of the Lindhard function accounts for forward and backward propagating bubbles and hence we are automatically taking into account the two diagrams depicted in fig. 5, where the proton of the ph excitation is an occupied state in diagram (a) while the neutron is the occupied state in diagram (b). It is straightforward to take into account the Δh excitation. It is sufficient to substitute U_N by $U_N + U_\Delta$, where U_Δ is the Lindhard function for Δh excitation conveniently normalized. Formulae for U_N, U_Δ with the normalization required here can be found in the Appendix of ref. [30].

The next step requires the evaluation of this vertex in the isospin state $T = 0$. The $T = 0$ state is

$$|\pi\pi, T = 0 \rangle = -\frac{1}{\sqrt{6}} |\pi^+(\vec{q})\pi^-(-\vec{q}) + \pi^-(\vec{q})\pi^+(-\vec{q}) + \pi^0(\vec{q})\pi^0(-\vec{q}) \rangle \quad (17)$$

where the phases and normalization are chosen as in [13]. The extra factor $\frac{1}{\sqrt{2}}$ in the normalization is chosen such as to preserve the closure sum, $\sum_{\vec{q}} |\langle \dots | = 1$, because, the $|\pi\pi, T = 0 \rangle$ is a symmetrical state.

By summing the contributions from the ph and Δh on the upper meson line we obtain

$$\tilde{t} = -\frac{1}{3f^4} \left(\frac{D+F}{2}\right)^2 \vec{q}^2 U(q_2) \quad (18)$$

where $\vec{q} = \vec{q}_1 = -\vec{q}_2$.

Next we turn our attention to another sort of diagram which we obtain from the consideration of the contact term in each one of the vertices of the one loop diagram. This is depicted in fig. 6. Its contribution to the $\pi^+\pi^- T$ matrix with a π^+ ph intermediate state is readily evaluated and one obtains,

$$\tilde{t}_{R,ph} = i\frac{1}{36f^6} \left(\frac{D+F}{2}\right)^2 \int \frac{d^4 q_1}{(2\pi)^4} \vec{q}_1^2 D_0(q_1) U_N(q_2) \quad (19)$$

where $D_0(q_1)$ is the pion propagator and $q_2 = k_1 + k_2 - q_1$.

Furthermore, substituting the $\pi^+ ph$ intermediate state by a $\pi^0 ph$ state leads to a similar contribution but substituting $\frac{1}{36}$ by $\frac{1}{18}$ in eq. (19), account taken of the symmetry of the intermediate state which introduces a relative factor $\frac{1}{2}$ since the diagram where the ph is excited in the lower one is topologically equivalent to the former one. One can work out the other combinations with $\pi^0\pi^0$ in the initial or final states and then evaluate the $T = 0$ contribution which is given by

$$\tilde{t}_R = i \frac{1}{9f^6} \left(\frac{D+F}{2} \right)^2 \int \frac{d^4 q_1}{(2\pi)^4} D_0(q_1) \vec{q}_1^2 U_N(q_2) \quad (20)$$

Once again, taking into account Δh excitation is straightforward and one simply substitutes U_N by $U_N + U_\Delta$ in eq. (20).

4 Off shell extrapolation of amplitudes and cancellations.

Let us come back to the diagram of fig. 2b. In the case of free pion scattering we could prove that the $\pi\pi$ amplitude in the loops factorized on-shell, and the off shell part went into renormalization of couplings and masses[13]. Here the presence of the ph excitation changes the analytical structure of the diagram and we must investigate what happens to the off shell extrapolation of the $\pi\pi$ amplitudes. For this purpose we recall that we shall be interested in the strength of the $\pi\pi$ system, which is related to ImT_{22} . If we look at the diagram of fig. 2b, the imaginary part can come, according to Cutkosky rules, when the two intermediate pions are placed on-shell or when the lower pion and the ph are placed on-shell. In both cases the lower pion with momentum q_1 is placed on-shell. The same occurs with the diagrams of fig. 4a,b. Thus, the off-shell $\pi\pi$ potential in those diagrams, with external pions placed on-shell, according to eqs. (4), (8), reads now

$$V_{off} = V_{on} + \frac{1}{3f^2} (q_2^2 - m_\pi^2) \quad (21)$$

The contribution of the diagram of fig. 2b to the $\pi\pi$ S = 0, T = 0 amplitude is given by

$$\begin{aligned} -it^{(1)} &= \int \frac{d^4 q_1}{(2\pi)^4} \frac{1}{f^2} \left\{ V_{on}^2 + \frac{2}{3f^2} V_{on} (q_2^2 - m_\pi^2) + \frac{1}{9f^4} (q_2^2 - m_\pi^2)^2 \right\} \\ &\times \left(\frac{D+F}{2} \right)^2 D_0^2(q_2) D_0(q_1) \vec{q}_2^2 U(q_2) \end{aligned} \quad (22)$$

On the other hand, the sum of the amplitudes of diagrams (a) and (b) of fig. 4, which contribute equally, is given by

$$\begin{aligned}
-it^{(2)} = & -2 \int \frac{d^4 q_1}{(2\pi)^4} \frac{1}{3f^4} \left(\frac{D+F}{2} \right)^2 \bar{q}_2^2 D_0(q_1) D_0(q_2) \{V_{on} + \frac{1}{3f^2} (q_2^2 - m_\pi^2)\} \\
& \times U(q_2)
\end{aligned} \tag{23}$$

It is interesting to note that the terms proportional to V_{on} in eq. (22) and eq. (23) cancel exactly. This leaves us with the term with V_{on}^2 in eq. (22) plus the terms proportional to $(q_2^2 - m_\pi^2)^2$ in eq. (22) and the one proportional to $(q_2^2 - m_\pi^2)$ in eq. (23). It is also interesting to note that these latter two terms have the same structure as the term \tilde{t}_R from eq. (20), corresponding to the diagram of fig. 6, and the sum of the three also cancels exactly.

In practical terms the situation has become rather easy. The terms of fig. 4 and 6 do not have to be evaluated and those of fig. 2 must be included but with $V_{\pi\pi}$ evaluated on-shell. These findings agree with the results of [31] which also show that the off shell contribution depends on the representation chosen while observable quantities should be independent of it.

The arguments can be extended to higher order loops of the type of fig. 2 and fig. 4, with the result that we must omit the terms of the type of fig. 4 and 6 and include only loops of the type of fig. 2 but with $V_{\pi\pi}$ on-shell. This allows the factorization of the potential outside the integrals and the Lippmann Schwinger equations are readily evaluated since they become algebraic equations like in the free $\pi\pi$ scattering case.

5 Coupled channel equations

We take as channels $\pi\pi$ and $K\bar{K}$ but do not renormalize the $K\bar{K}$ system as discussed above. The series of terms in the Lippmann Schwinger eqns., which include the potential, the terms of fig. 2 and higher order iterations of that type, including also free $K\bar{K}$ intermediate states, is given by

$$T_{22} = V_{22} + V_{21}G_{11}t_{12} + V_{22}\tilde{G}_{22}T_{22} \tag{24}$$

where only T_{22} and \tilde{G}_{22} are renormalized in the medium. The other quantities are evaluated in free space and are taken from ref. [13]. We can obtain T_{22} from eq. (24)

$$T_{22} = \frac{V_{22} + V_{21}G_{11}t_{12}}{1 - V_{22}\tilde{G}_{22}} \tag{25}$$

The integral of the two pion propagators in the medium, \tilde{G}_{22} , is then given by

$$\tilde{G}_{22} = i \int \frac{d^4 q}{(2\pi)^4} D(q)D(P - q) \tag{26}$$

with

$$V_{22} = V_{22,on} = -\frac{1}{9f^2}\left(9s + \frac{15m_\pi^2}{2} - 12m_\pi^2\right) \quad (27)$$

and

$$D(q) = \frac{1}{q^2 - m_\pi^2 - \Pi(q)} \quad (28)$$

where $\Pi(q)$ is the pion selfenergy in the medium

$$\Pi(q) = \frac{\left(\frac{D+F}{2f}\right)^2 \vec{q}^2 U(q)}{1 - \left(\frac{D+F}{2f}\right)^2 g' U(q)} \quad (29)$$

with g' the Landau-Migdal parameter, which we take as $g' = 0.7$.

When including the pion selfenergy in eq. (28) we also go beyond the lowest order diagrams in density that we have discussed in detail, but this is the appropriate way to take the higher order diagrams into account.

We have also included the pion selfenergy accounting for $2p2h$ excitation. Since we are concerned mostly around the pion threshold region ($\sqrt{s} \sim 2m_\pi$) we have taken this selfenergy from pionic atoms. The procedure is discussed in detail in [32] and it amounts to substituting in eq. (29)

$$\left(\frac{D+F}{2f}\right)^2 U(q) \rightarrow \left(\frac{D+F}{2f}\right)^2 U(q) - 4\pi C_0^* \rho^2 \quad (30)$$

with ρ the nuclear density and

$$C_0^* = (0.105 + i 0.096) m_\pi^{-6} \quad (31)$$

It is interesting to note that eq. (25) leads to a zero very close to the one where $V_{22} = 0$ (Adler zero) since the second term in the numerator of eq. (25), involving kaon loops, is negligible around that energy. Hence our approach fulfils the minimal chiral constraints (MCC) of ref. [10] even in the presence of the nuclear medium.

6 Results and discussion

In fig. 7 we show ImT_{22} as a function of the energy for different values of k_F , the Fermi momentum. The results show a reduction of strength below the ‘ σ ’ region and an accumulation of strength at low energies around the pion threshold. The results obtained omitting the $2p2h$ part of the pion selfenergy are qualitatively similar to those in fig. 7 at energies below 600 MeV. In the region close to the dip of the $f_0(980)$ resonance the results including the $2p2h$ part are about 30% smaller than those omitting them. At these energies a more realistic evaluation of this part would be needed but since we are not concerned about this region we do not elaborate further on the issue.

The results obtained resemble very much those shown in fig. 12 of ref. [8] and particularly those of fig. 3 of [33], where first attempts to relate the accumulated strength around pion threshold to the experiment of [3] are done.

The association of the peaks found here to the extra strength around pion threshold found in the experiment at small pion pair invariant mass [3] is not straightforward. Indeed, even if this invariant mass is small, the pion pair moves with some momentum. Here we have studied the $\pi\pi$ system at rest in nuclear matter and there could be differences for a $\pi\pi$ pair moving with respect to the rest frame of the Fermi sea. Yet the steps taken in [33] are encouraging and more work along these lines would be welcome.

It should also be pointed out that we have selected the diagrams for $\pi\pi$ free scattering and carried out the renormalization for the mesons while at the same time have kept the partner terms which appear at the same order of the chiral counting and make the scheme invariant under unitary transformations of the fields. This would in principle guarantee that relationships like Ward identities and other, which are sometimes used in the study of the interaction of ρ -mesons with matter [34], would be satisfied. Alternative methods to test Ward identities can be made using the master formula of [35], where the most general amplitude for $\pi\pi$ scattering satisfying chiral constraints is derived and expressed in terms of form factors and polarization functions. The use of resonance saturation for the evaluation of these latter magnitudes leads to a consistency check of the master formula [35]. Our approach [13, 15] leads dynamically to the different meson meson resonances and would naturally provide the resonance contribution to those functions, hence indirectly fulfilling the test done in [35].

On the other hand, one can think of other many body diagrams which in principle contribute to the process. Think for instance of a baryon box diagram with 4 meson legs attached at different points of it, or the same box diagram with two pairs of mesons attached at two points, etc. These diagrams require the use of other terms of the chiral Lagrangians used above and do not interfere with the counting done so far. Furthermore, inspection of these diagrams proves that sometimes the isoscalar πN amplitude is involved, which is quite small on shell, although it can be appreciably modified in some off shell situations. Other times one meets with the p -wave πN interaction, while we are interested in s-wave propagation. In most cases, like in those box diagrams, a ph is forced to propagate carrying zero momentum and the two meson energy, which places it very far off shell, etc. These are qualitative arguments which indicate small contributions from such terms and would support our choice of many body diagrams as the relevant set for the process studied. However, detailed studies of these alternative many body mechanisms would be welcome.

7 Conclusions

We have performed calculations of the $\pi\pi$ scalar-isoscalar amplitude in a nuclear medium starting from the standard chiral Lagrangians and using a unitary framework with coupled channels which proved rather successful in describing the meson-meson interaction in the scalar sector.

Compared to other schemes that impose minimal constraints of chiral symmetry, essentially the vanishing of the $\pi\pi$ amplitude in the limit of $m_\pi \rightarrow 0$, our scheme uses the input of the standard chiral Lagrangians and generates different terms, in the expansion on the number of meson fields, which appear on the same footing in the $\pi\pi$ amplitude in the presence of a nuclear medium. In this way, some terms related to the contact term $\pi\pi\pi NN$, which appears in the $\pi N \rightarrow \pi\pi N$ reaction, and which are new with respect to previous approaches, are generated here. Simultaneously, the off-shell extrapolation of the chiral $\pi\pi$ amplitudes is used and it is shown to produce cancellations with the terms coming from the contact vertices, with the remarkable result that only the one shell part of the $0(p^2)$ meson meson amplitudes is needed, like in the case of free meson scattering.

This shows the usefulness of working explicitly with chiral Lagrangians in order to find out those subtle cancellations. Our results show a reduction of strength of ImT_{22} in the ' σ ' region and an accumulation of strength close to pion threshold which are features shared by most of the approaches.

Quantitatively our results resemble very much some results in the literature which use models imposing minimal chiral constraints. Among a large variety of prescriptions used in the past to account for $\pi\pi$ interaction in the medium, the present approach offers a cleaner link to chiral dynamics. This has been made possible by the work of [13] which could combine exact unitarity with the input of the chiral Lagrangians, describing accurately the free meson meson interaction. Work along these lines in the study of the modification of the meson meson interaction in a nuclear medium for other channels is equally possible and would be welcome.

On the other hand, the clear accumulation of strength around pion threshold (even without singularities as claimed in some approaches) which is also shared by some models, is an appealing feature that most probably can be linked to present experiments showing enhanced distributions of $\pi\pi$ invariant mass in $T = 0$ around pion threshold. Further investigation along these lines is another of the challenging tasks ahead.

Acknowledgements:

We would like to thank J. A. Oller for help and discussions. Discussions with Z. Aouissat, B. Friman, J. Wambach, A. Wirzba, G. Chanfray and I. Zahed are also acknowledged. One of us, H. C. Chiang wishes to acknowledge financial support from the Ministerio de Educación y Cultura in his sabbatical

stay in the University of Valencia. This work is partly supported by DGICYT contract number PB96-0753.

Appendix

Matrix elements of the contact terms of fig. 8 in the meson-meson CM frame ($\vec{k}_1 + \vec{k}_2 = 0$):

$$iL_a = \frac{D+F}{2} \frac{\sqrt{2}}{12f^3} 2 \vec{\sigma} \cdot (3\vec{k}_1 + \vec{q}_1), \quad (32)$$

$$iL_b = \frac{D+F}{2} \frac{\sqrt{2}}{12f^3} 2 \vec{\sigma} \cdot (3\vec{k}_2 + \vec{q}_2), \quad (33)$$

$$iL_c = \pm \frac{D+F}{2} \frac{\sqrt{2}}{12f^3} \frac{1}{\sqrt{2}} 4 \vec{\sigma} \cdot \vec{q}_1, \quad (34)$$

with a plus(minus) sign for the proton(neutron) case,

$$iL_d = \frac{D+F}{2} \frac{\sqrt{2}}{12f^3} 4 \vec{\sigma} \cdot \vec{q}_1, \quad (35)$$

$$iL_e = \frac{D+F}{2} \frac{\sqrt{2}}{12f^3} 4 \vec{\sigma} \cdot \vec{q}_2, \quad (36)$$

$$iL_f = 0 \quad (37)$$

Figure captions:

Fig. 1:

Diagrammatic representation of the $\pi\pi$ scattering matrix contained in the Lippmann Schwinger coupled channel equations.

Fig. 2:

Terms appearing in the scattering matrix allowing the pions excite ph and Δh components.

Fig. 3:

Pion pole (a) and contact term (b), appearing in the construction of the $\pi N \rightarrow \pi\pi N$ amplitude.

Fig. 4:

Terms of the $\pi\pi$ scattering series in the nuclear medium tied up to the contact terms of fig. 3.

Fig. 5:

Direct and crossed ph excitation terms contained in the modified 4π vertex, accounted for by means of the ordinary Lindhard function.

Fig. 6:

Diagram tied to the contact term of fig. 3b, allowing for ph excitation and a pion in the intermediate state.

Fig. 7:

$\text{Im } T_{22}$ for $\pi\pi \rightarrow \pi\pi$ scattering in $J = T = 0$ (T_{00} in the figure) in the nuclear medium for different values of k_F versus the CM energy of the pion pair. The labels correspond to the values of k_F in MeV.

Fig. 8:

Contact terms appearing in the construction of the $\pi N \rightarrow \pi\pi N$ amplitude.

References

- [1] P. Schuck, W. Nörenberg and G. Chanfray, *Z. Phys.* A330 (1988) 119.
- [2] N. Grion et al., *Phys. Rev. Lett.* 59 (1987) 1080.
- [3] F. Bonutti et al., *Phys. Rev. Lett.* 77 (1996) 603.
- [4] G. Chanfray, Z. Aouissat, P. Schuck and W. Nörenberg, *Phys. Lett.* B256 (1991) 325.
- [5] J.A. Johnstone and T.S. H. Lee, *Phys. Rev.* C34 (1986) 243.
- [6] J. W. Durso, A. D. Jackson and B. J. Verwest, *Nucl. Phys.* A345 (1980) 471.
- [7] Z. Aouissat, G. Chanfray and P. Schuck, *Mod. Phys. Lett.* A8 (1993) 1379.
- [8] Z. Aouissat, R. Rapp, G. Chanfray, P. Schuck and J. Wambach, *Nucl. Phys.* A581 (1995) 471.
- [9] D. Lohse, J.W. Durso, K. Holinde and J. Speth, *Phys. Lett.* B234 (1989) 235; *Nucl. Phys.* A516 (1990) 513.
- [10] R. Rapp, J.W. Durso and J. Wambach, *Nucl. Phys.* A596 (1996) 436.
- [11] J. Gasser and H. Leutwyler, *Nucl. Phys.* B250 (1985) 465.
- [12] A. Dobado, M.J. Herrero and T.N. Truong, *Phys. Lett.* B235 (1990) 129; A. Dobado and J.R. Pelaez, *Phys. Rev.* D47 (1992) 4883; *ibid*, *Phys. Rev.* D56 (1997) 3057.
- [13] J.A. Oller and E. Oset, *Nucl. Phys.* A620 (1997) 438.
- [14] T. N. Truong, *Phys. Rev. Lett.* 61 (1988) 2526; *ibid* 67 (1991) 2260.
- [15] J. A. Oller, E. Oset and J. R. Peláez, *Phys. Rev. Lett.* 80 (1998) 2452.
- [16] J. Nieves and E. Ruiz-Arriola, *nucl-th/9807035*.
- [17] S. Weinberg, *Phys. Rev. Lett.* 17 (1966) 616; *Phys. Lett.* 18 (1967) 188.
- [18] M.G. Olsson and L. Turner, *Phys. Rev. Lett.* 20 (1968) 1127.
- [19] E. Oset, C. García-Recio and J. Nieves, *Nucl. Phys.* A584 (1995) 653.
- [20] U. G. Meissner, E. Oset and A. Pich, *Phys. Lett.* B353 (1995) 161.
- [21] E. Oset and M.J. Vicente Vacas, *Nucl. Phys.* A446 (1985) 584.

- [22] O. Jaekel, M. Dillig, C. A. Z. Vasconcelos, Nucl. Phys. A541 (1992)673. 584.
- [23] V. Bernard, N. Kaiser and U.G. Meissner, Nucl. Phys. B457 (1995) 147; ibid A619 (1997) 261.
- [24] T.S. Jensen and A.F. Miranda, Phys. Rev. C55 (1997) 1039.
- [25] E. Oset and M.J. Vicente-Vacas, Phys. Lett. B386 (1996) 39.
- [26] U.G. Meissner, Rep. Prog. Phys. 56 (1993) 903; V. Bernard, N. Kaiser and U.G. Meissner, Int. J. Mod. Phys. E4 (1995) 193.
- [27] A. Pich, Rep. Prog. Phys. 58 (1995) 563.
- [28] G. Ecker, Prog. Part. Nucl. Phys. 35 (1995) 1.
- [29] A. L. Fetter and J.D. Walecka, Quantum Theory of many-particle systems (McGraw-Hill, New York, 1971).
- [30] E. Oset, P. Fernández de Córdoba, L.L. Salcedo and R. Brockmann, Phys. Reports 188 (1990) 79.
- [31] G. Chanfray and D. Davesne, nucl-th/9806086.
- [32] A. Ramos, E. Oset and L.L. Salcedo, Phys. Rev. C50 (1994) 2314.
- [33] Z. Aouissat et al., nucl-th/9806069.
- [34] M. Hermann, B.L. Friman and W. Nörenberg, Nucl. Phys. A560 (1993) 411.
- [35] J.V. Steele, H. Yamagishi and I. Zahed, Nucl. Phys. A615 (1997) 305.

$$\mathbf{T}_{22} = \text{[Diagram 1]} + \text{[Diagram 2]} + \text{[Diagram 3]} + \text{[Diagram 4]} + \dots$$

The figure shows the expansion of the transition amplitude \mathbf{T}_{22} into a series of diagrams:

- Diagram 1:** A four-point vertex where four dashed lines meet at a central point.
- Diagram 2:** A loop of dashed lines with two external dashed lines. The top loop is labeled q and the bottom loop is labeled $P - q$.
- Diagram 3:** A loop of solid lines with two external dashed lines. The top loop is labeled K and the bottom loop is labeled \bar{K} .
- Diagram 4:** A chain of two dashed loops with four external dashed lines.

 The series is followed by an ellipsis \dots .

Fig. 1

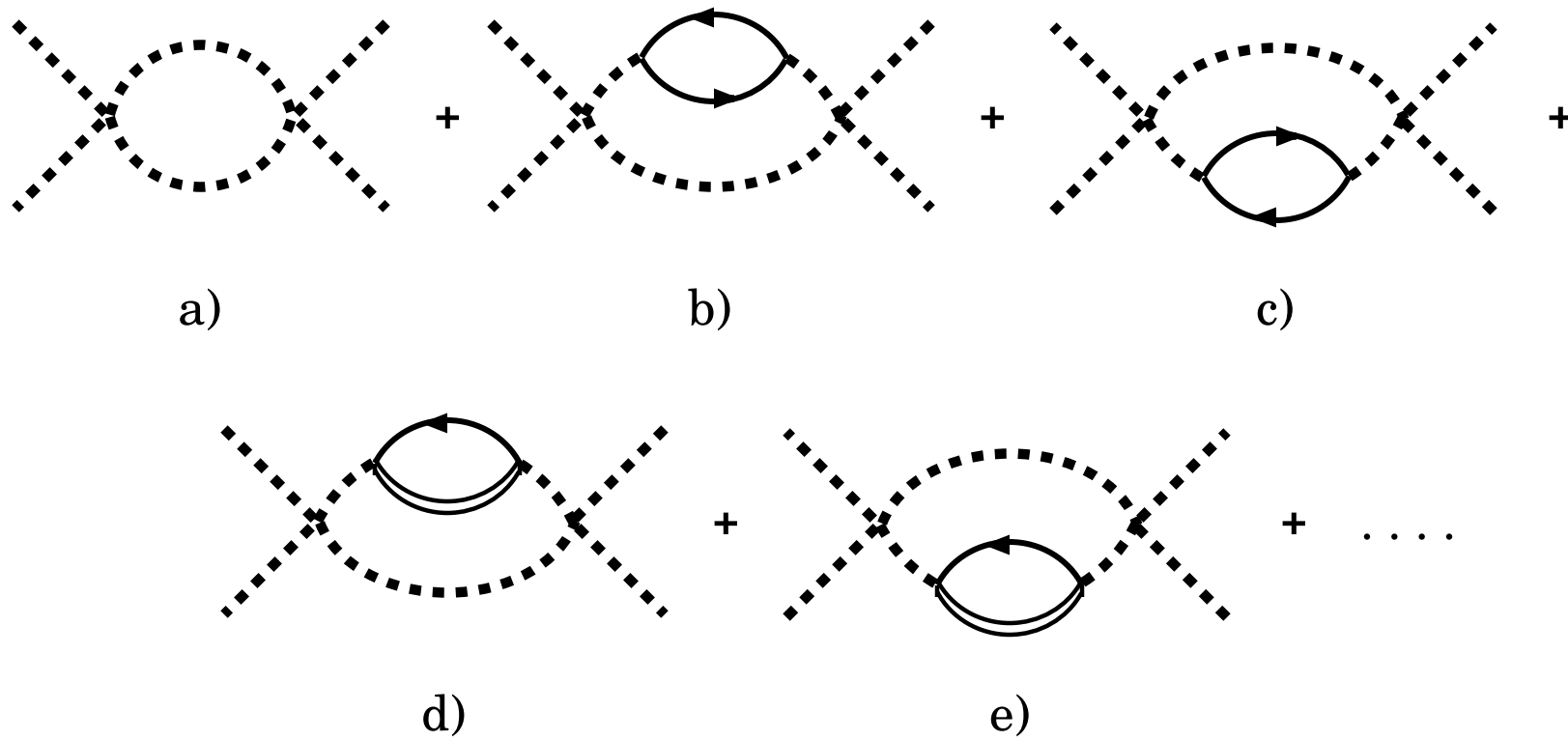
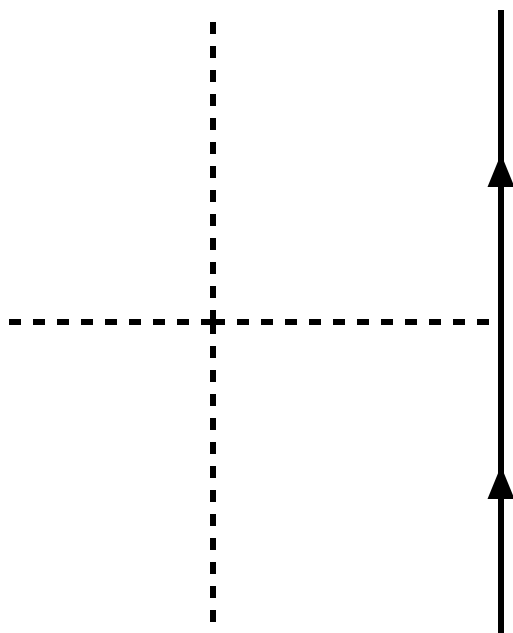
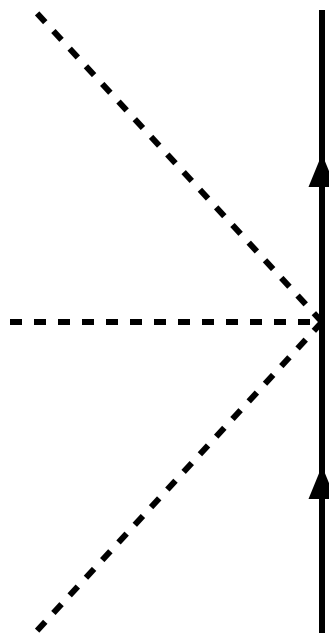


Fig. 2



a)



b)

Fig. 3

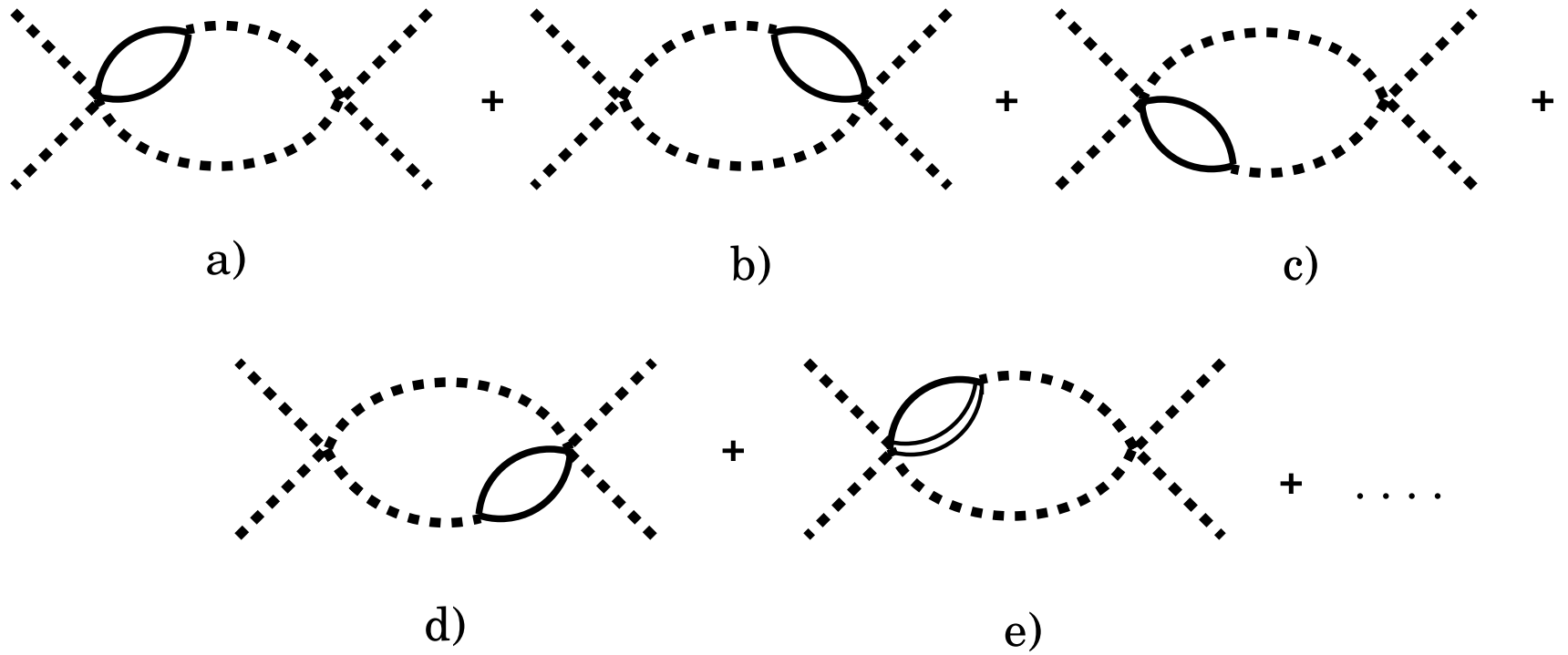


Fig. 4

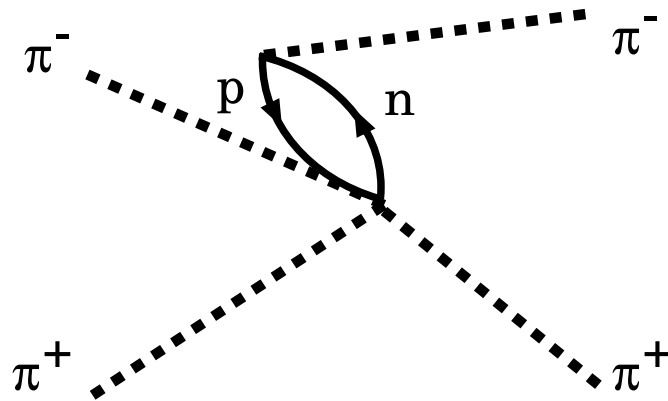
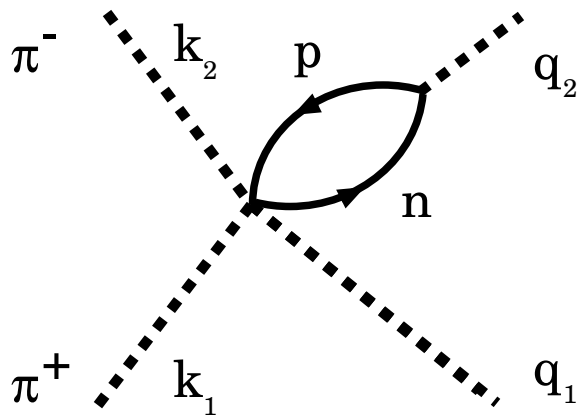


Fig. 5

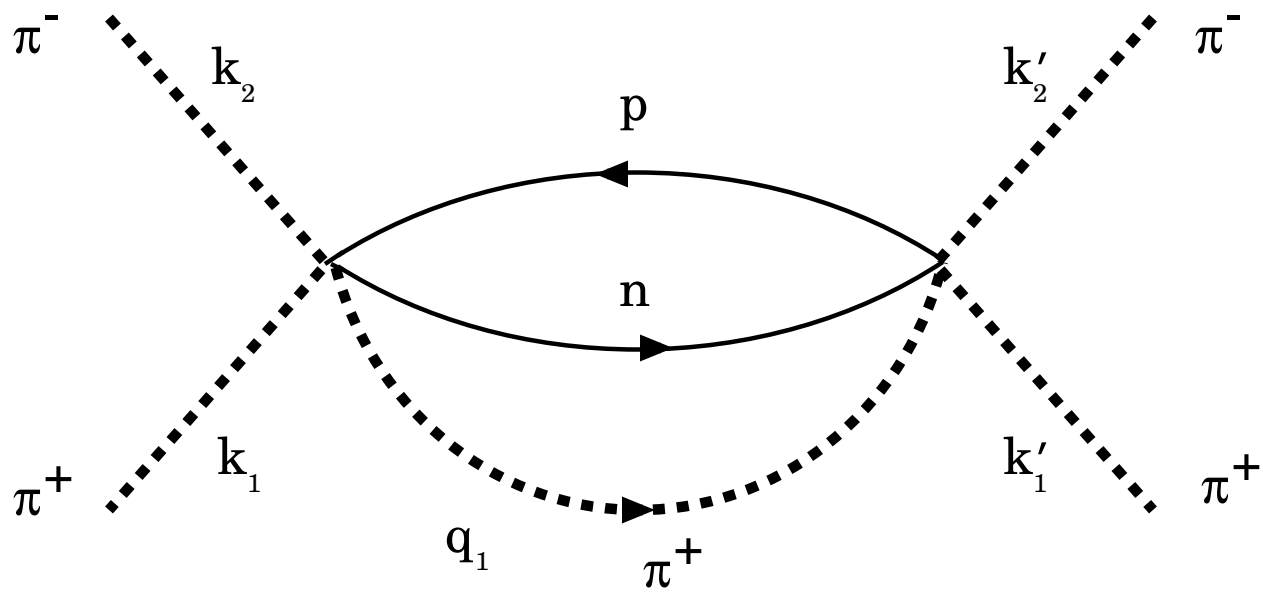


Fig. 6

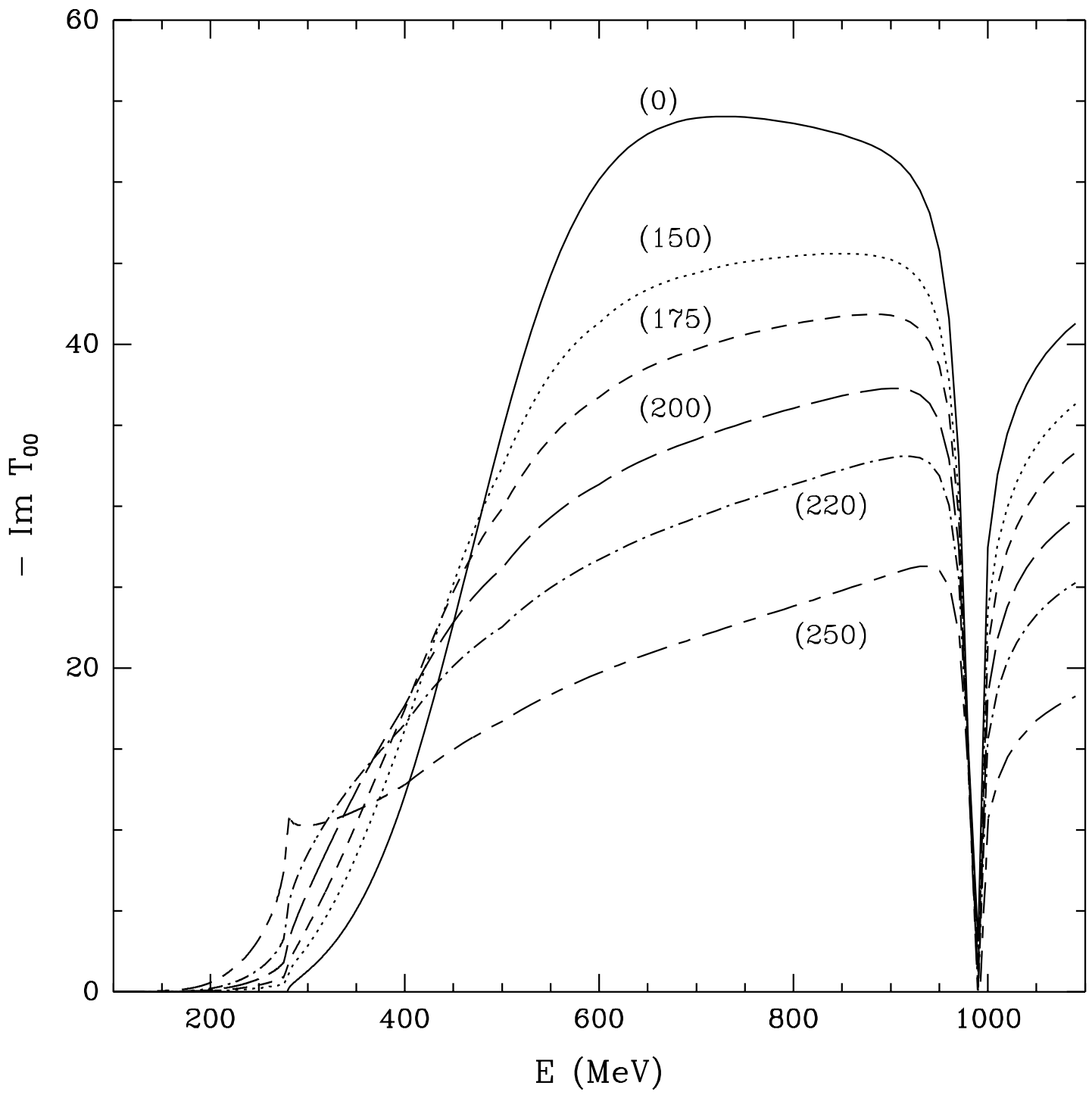
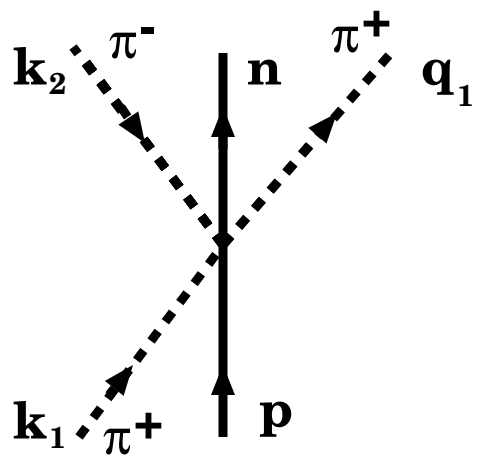
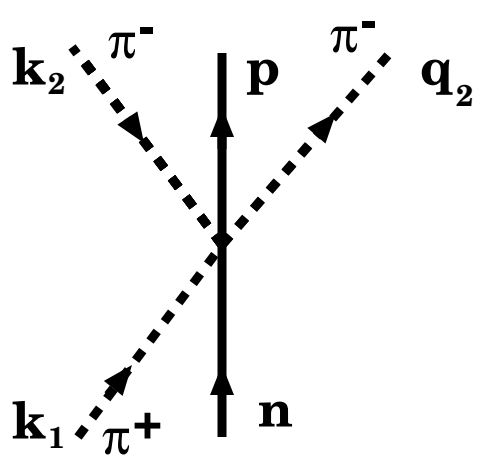


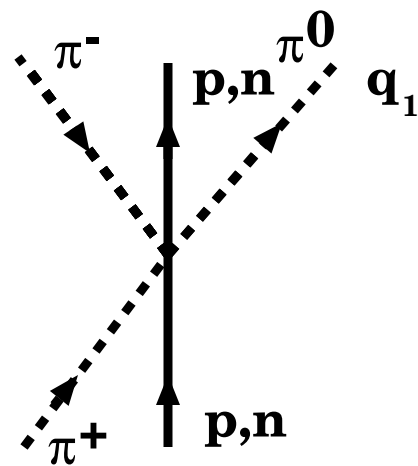
Fig. (7)



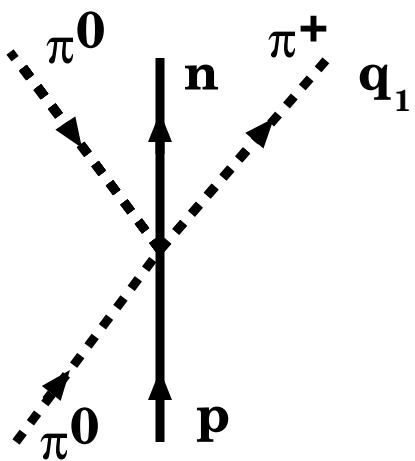
a)



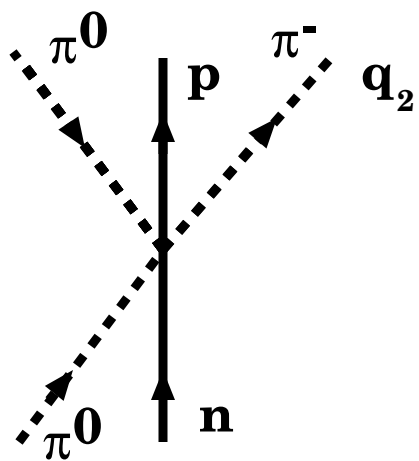
b)



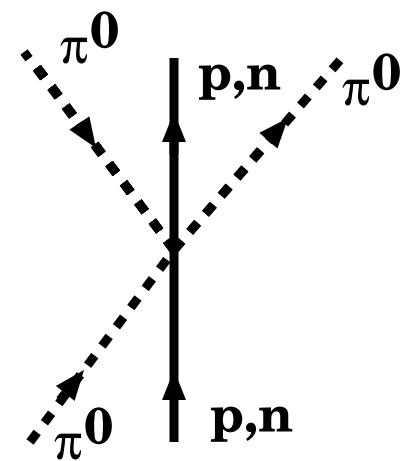
c)



d)



e)



f)

Fig. 8